

Simulation of acoustic propagation along a section in the Western Bay of Bengal

T.V. RAMANA MURTY, Y.K. SOMAYAJULU and J.S. SASTRY
National Institute of Oceanography, Dona Paula, Goa-403 004.

The mean sound speed profiles constructed for the winter and premonsoon seasons (January, February and March/April 1988) from CTD temperature, salinity profiles along a section in the western Bay of Bengal (off Madras) are utilised to carry out acoustic ray tracing for determining the set of rays connecting the given source and the receiver locations in the deep sound channel. The acoustic parameters such as the geometric path, ray identifier, turning points, travel time and signal strength are computed and presented in the form of tables and plots. Noticeable variations in the simulated propagation characteristics are caused by cooling of the waters of the wave guide from winter to the premonsoon. The pulse arrival times are found to be resolvable during both the periods. The flight of the rays are slower (by about 170 ms) and the intensity losses are higher (-103 dB as against -97 dB) during premonsoon compared to the winter. The signal strengths varied from about -95 dB to -109 dB between the two seasons over a range of 300 kms.

Introduction

Ocean Acoustic Tomography deals with screening or examination of the interior weather of the oceans achieved by measuring travel times of acoustic rays emanating from a source and reaching a distant receiver within the ocean volume. The perturbations in travel times between the measured and the computed ones are made use of to reconstruct the sound speed field by proper application of Geophysical inversion methods.

The acoustic energy transmitted from a source is usually described in terms of rays whose characteristics are governed by the index of refraction. Each ray travels along a unique path as determined by the angle of emergence at its source. A single pulse emitted at the source reaches the receiver as an ensemble of multiple rays whose arrival times differ by few milliseconds. The identification of ray arrivals reaching the receiver through multiple paths forms the study of the direct problem and leads to the development of data kernel for purposes of application of Generalized Inverse theories.

As a part of the investigations aimed at developing techniques for remote sensing of the ocean interior, simulation studies on acoustic propagation are taken up. The article highlights the salient features of the results of the study of propagation along a section in the western Bay of Bengal.

The environmental data collected utilising MICOM STD during the two scientific cruises in the Bay of Bengal (Fig. 1), during January/February and March/April, 1988 form the input for sound speed computations utilising the software detailed elsewhere (Ramana Murty *et. al.*)¹. For sound speed computations the following empirical formulae (Chen & Millero)² are used.

$$c(s, t, p) = c_w(t, p) + A(t, p)s + B(t, p)s^{3/2} + D(t, p)s^2 \quad \dots(1)$$

where p = pressure (in decibars),
 t = temperature (deg. celcius)
 s = salinity (pss)
 c = sound speed (meters/sec.)

In the above equation the first term on the right

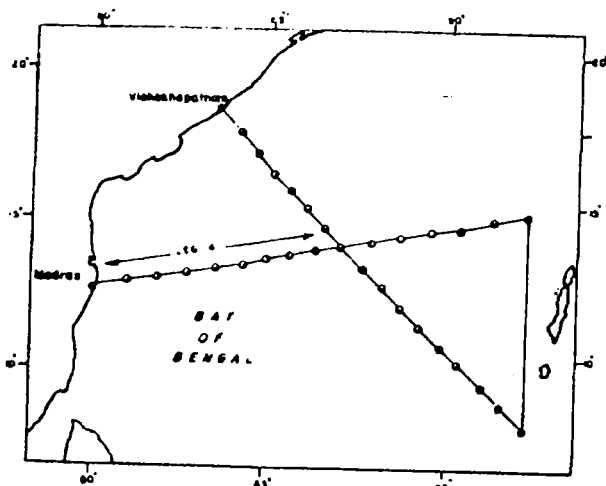


Fig. 1. Map showing station locations

hand side represents fifth order polynomial in temperature and pressure whereas the remaining terms are of fourth order. The coefficients of the polynomials have been detailed in the paper by Chen & Millero.

Ray acoustics

Following Arthur *et. al.*³, the ray geometry is governed by the equations given below :

$$dx = \cos \theta ds \quad \dots(2)$$

$$dy = \sin \theta ds \quad \dots(3)$$

$$d\theta = -c^{-1} \cos \theta \partial c / \partial y ds \quad \dots(4)$$

In the above equations x and y represent horizontal and vertical coordinates, θ is the angle of the ray w.r.t. the horizontal and s is the arc length along the ray which is chosen to sample well enough the sound speed and its gradients for determining ray parameters. $\partial c / \partial y$ is the vertical sound speed gradient.

For a given ray the geometric path can be computed and source-to-receiver travel time is estimated using the equation

$$T_i = \int [c_o(s)]^{-1} ds \quad \dots(5)$$

ray path i

$i=1, N$ where N is the number of rays. The above integration is carried out along the ray path.

Expressions of Krol⁴, Moler and Solomon⁵ are used in the computation of acoustic intensity. The

calculations are based on the assumption that (i) changes in the intensity occur only due to contraction or expansion of the ray tube and (ii) the power transmitted between two adjacent rays (separated by $1/100$ of a degree) is conserved.

The acoustic intensity at any point along the ray path is thus given by

$$\text{Intensity} = I(X)/I_o = \sin \theta_o / X \cos \theta \frac{\Delta Y}{\Delta \theta_o} \quad (6)$$

where I_o : the reference intensity at the source,

θ_o : Eigen ray angle at the source with reference to the horizontal

θ : Ray angle at the point of measurement w.r.t. the horizontal

X : Distance from the source to the point of measurement

ΔY : Vertical distance at the point of measurement between the eigen ray and the ray in its immediate vicinity

$\Delta \theta_o$: Angle between the eigen ray and the ray in its immediate vicinity at the source

The above expression will not hold good mathematically as $\Delta Y \rightarrow 0$ and only the previous value is considered for computational continuity.

Considering the phase shift for any given frequency the intensity is given by

$$I/I_o = \left| \sum_k P_k e^{i \pi f (t_k)} \right|^2 \quad \dots(7)$$

$$\sum_j P_j P_k \cos (2\pi f (t_j - t_k))$$

where $P_k = (I_k(x)/I_o)$ and t_k are the relative pressures

and arrival times of the eigen rays and have wider applications in signal detection.

Results and Discussions

The average sound speed profile is constructed from the computed sound speed profiles at several stations along the section. The mean profiles for the winter and premonsoon show higher sound speed values of about 1537.5 m/sec and 1544.7 m/sec. respectively at the surface while at the bottom the values are

Table 1. Acoustic ray parameters for a) winter and b) premonsoon.

S. Ang (Deg)	Loop Len (Km.)	Era Len (Km.)	No. Loops & R. Ident	T. Dep 1 (M)	T. Vel 1 (M/S)	T. Dep 2 (M)	T. Vel 2 (M/S)	P. Len (Km)	T. Time (Sec)	R. Ang (Deg)	R. Dep (M)
(a)											
5.7806	65.610	37.559	4 (5,-4)	-348.09	1500.59	-2550.91	1500.58	301.022	201.1541	-5.715	-1799.20
1.0751	51.114	44.430	5 (6,-6)	-1538.03	1493.22	-1826.76	1493.22	300.223	201.0725	.557	-1800.86
.9485	52.291	38.547	5 (6,-5)	-1554.94	1493.17	-1805.77	1493.17	300.217	201.0721	-.278	-1799.92
-1.4697	98.572	4.284	3 (3,-3)	-1889.25	1493.45	-1735.56	1493.45	300.225	201.0450	-1.160	-1800.32
-4.5135	68.741	25.037	4 (4,-5)	-2312.05	1497.60	-306.64	1497.60	300.662	201.0712	4.413	-1800.06
-5.4564	68.190	22.242	4 (4,-5)	-2486.38	1499.76	-375.86	1499.76	300.883	201.0785	5.368	-1800.95
(b)											
S. Ang (Deg)	Loop Len (Km.)	Era Len (Km.)	No. Loops & R. Ident	T. Dep 1 (M)	T. Vel 1 (M/S)	T. Dep 2 (M)	T. Vel 2 (M/S)	P. Len (Km)	T. Time (Sec)	R. Ang (Deg)	R. Dep (M)
6.9043	60.165	59.340	4 (5,-5)	-265.32	1502.31	-2709.45	1502.32	301.377	201.3976	6.750	-1799.30
5.4344	65.064	39.745	4 (5,-4)	-408.54	1498.15	-2400.66	1498.14	300.903	201.3217	-5.294	-1799.61
4.0452	64.043	43.827	4 (5,-4)	-672.43	1495.13	-2145.58	1495.13	300.596	201.3150	-3.855	-1800.34
3.4440	63.826	44.698	4 (5,-4)	-731.20	1494.11	-2059.65	1494.11	300.494	201.3155	-3.235	-1800.20
-7.0480	59.837	.816	5 (5,-5)	-2740.91	1502.76	-259.1	1502.74	301.434	201.4137	-6.936	-1800.27

Table 2. Ray arrival times and their intensity levels at the receiver (a) winter and (b) premonsoon.

S. No.	Source ANG. (deg)	Travel Time (sec)	I (X)/I ₀	Intensity (dB)
(a)				
1.	5.7806	.20115170E+03	.45867800E-10	-.10338490E+03
2.	1.0751	.20107250E+03	.84957290E-10	-.10070800E+03
3.	.9485	.20107210E+03	.18253380E-09	-.97386570E+02
4.	-1.4697	.20104590E+03	.12374540E-10	-.10907470E+03
5.	-4.5135	.20106920E+03	.16841920E-09	-.97736080E+02
6.	-5.4564	.20108000E+03	.29423190E-09	-.95313100E+02
(b)				
S. No.	Source Ang. (deg)	Travel Time (sec)	I (X)/I ₀	Intensity (dB)
1.	6.9043	.20139510E+03	.35277810E-09	-.94524990E+02
2.	5.4344	.20132060E+03	.19126370E-09	-.97183680E+02
3.	4.0452	.20131610E+03	.22374330E-09	-.96512210E+02
4.	3.4440	.20131490E+03	.25676230E-09	-.95904690E+02
5.	-7.0480	.20141560E+03	.19259420E-09	-.97153560E+02

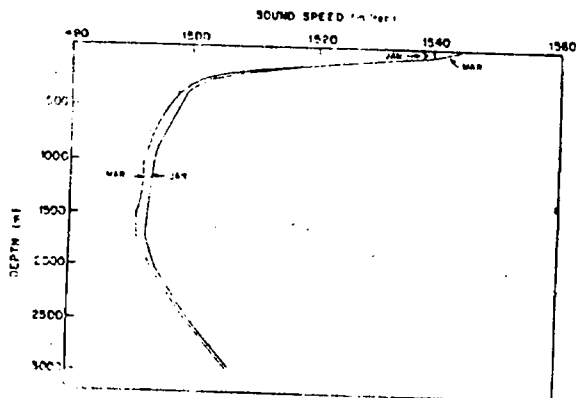


Fig. 2. Average sound speed profiles along the section.

1506.7 m/sec and 1506.2 m/sec. A marked variation in the sound speed between the two seasons is clearly seen in Fig 2.

The rays connecting the source and the receiver separated by 300 kms are depicted in Fig 3 and the various ray parameters computed are shown in Table 1. Rays emanating from the source at different emergence angles show variations in lengths of the ray loop (comprising one upper and one lower loops) which range between 51 and 98 kms. The number of loops vary from 3 to 5. The ray turning depths, the number of turnovers/turnunders and the sound speeds at the turning points are indicated in the table. The total path lengths along different rays, the travel times and the ray arrival angles are also presented. The time spans between the first and the last arrival at the receiver are found to spread over 110 ms and 100 ms during winter and premonsoon respectively.

The ray path lengths of different rays are tabulated layer wise. The information is the pre-requisite to construct the generalized inverse operators to operate

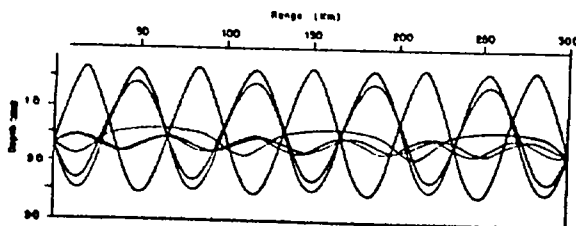


Fig. 3. Acoustic rays connecting the source and the receiver.

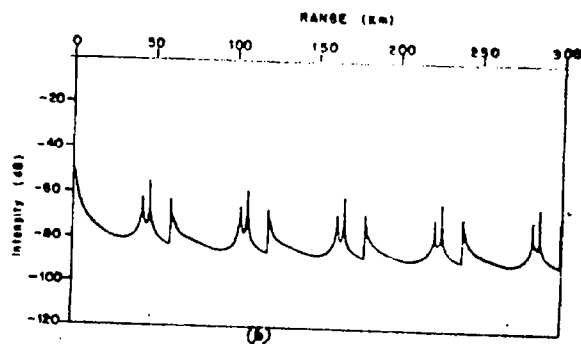
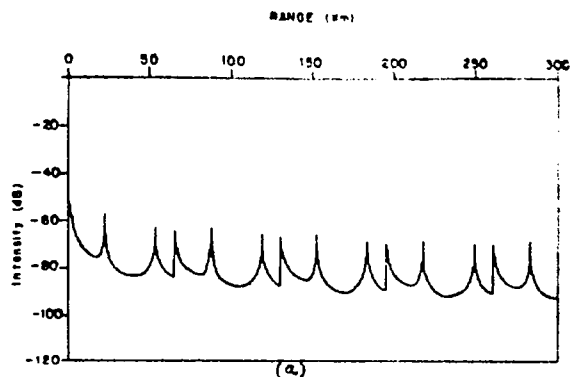


Fig. 4. Intensity levels versus range plots for winter and premonsoon seasons.

on travel time perturbations to get the model parameter anomalies.

The computed intensities along rays emanating at nearly same angles of emergence at the source during winter and the premonsoon are plotted against range and are shown in Fig. 4(a) and (b). The intensity levels of different rays reaching the receiver are presented in Table 2 (a) and (b). The intensity levels vary between -55 and -85 dB (during winter) and -55 and -90 dB (during premonsoon) and shows a linearly decreasing trend towards the receiver. The presence of multiple peaks in intensity versus range graph provides information on small scale features. The convergence zones could be identified by the larger peaks in this distribution. The intensity at the receiver (considering the phase shift due to multiple ray arrivals) over different frequencies for both the seasons is presented in Fig. 5

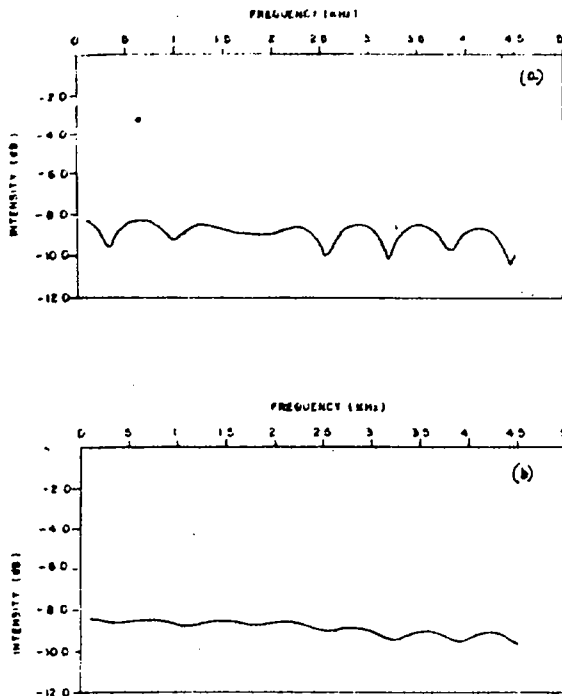


Fig. 5. Intensity levels (with phase) versus frequency at the receiver during winter and premonsoon.

(a) and (b). During winter the intensity level is stable with variation in source frequency while during premonsoon intensity levels showed fluctuations for different frequencies.

This article outlines information about resolvable travel times and the signal strengths. The flight time during winter is longer and true for all source—

receiver configurations. The seasonal mesoscale variability could be examined through arrival sequence of the eigen rays at the receivers which are resolvable in both seasons (approximately 197 millisecc).

Conclusions

(1) The time of flight of eigen rays during winter is more than that of the premonsoon season. The seasonal mesoscale variability can be examined through arrival sequence of the eigen rays spread over 170 ms at the receivers which are clearly resolvable in both the seasons.

(2) The signal strengths varied from -95 dB to -109 dB between the two seasons over the range of 300 km. Thus the intensity levels are higher in winter compared to premonsoon season.

Acknowledgements

The authors are thankful to the Director, NIO for his keen interest in this study. They acknowledge the help of D.O.D., Govt. of India, New Delhi for the grants given to the project.

References

1. Ramana Murty TV, Somayajulu YK and Gopala Krishna VV. *OCEAN—A Comprehensive Program for the Computation of Physical Parameters*, 1985 (Unpublished manuscript).
2. Chen CT and Miller FJ, *Acoust Soc Am* 62 (1977) 1129.
3. Arthur RS, Munk WH and Isaacs JD, *Trans Am Geophys Un* 33 (1952) 855.
4. Krul HR, *J Acoust Soc Am* 53 (1973) 864.
5. Moler CB and Solomon LP, *J Acoust Soc Am* 48 (1970) 739.